ce/papers Proceedings in civil engineering

Ernst & Sohn A Wiley Brand

ORIGINAL ARTICLE

eurosteel AMSTERDAM 2023

Ernst & Sohn A Wiley Brand

Specific distortion-induced fatigue failure at main girders of a railway bridge – efficiency of different reinforcements based on strain measurements

Harald Unterweger | Christoph Derler

Correspondence

Harald Unterweger
Graz University of Technology
Institute for Steel Structures
Lessingstraße 25
8010 Graz
Email: harald.unterweger@tugraz.at

Abstract

At the main girders of a three span continuous girder railway bridge, built in the 1960s, through-thickness cracks were detected in the web, at the location of the transverse stiffener to main girder connections. The transverse stiffeners are not welded to the girder flange, in order to increase their fatigue resistance. Instead, fitting strips between the stiffeners and the bottom flanges were used.

First of all, the paper presents the results of local strain measurements at the original detail, without any reinforcement, for individual train passages. These results confirm a distortion-induced fatigue failure, due to an unexpected high-frequency oscillation of the web plate. Based on that, three different types of reinforcement were developed and installed at the bridge. For each type of reinforcement further strain measurements were done during regular train service. Also, a weigh-in-motion-system was installed, to specify a representative passenger and freight train each. From the local strain measurements, during the passage of these two trains, the stress-spectra were evaluated for all three types of reinforcement. Furthermore, existing fatigue test data of a similar connection detail from the literature were re-assessed in order to provide an accurate fatigue resistance for the damage accumulation. The comparison of the evaluated fatigue damage of these individual stress spectra indicates the efficiency of each type of reinforcement.

Finally, also representative reduction factors of the initial stress ranges without reinforcement, were developed for each type of reinforcement. This allows a more generalized assessment, regarding the efficiency of the different types of reinforcement, not just valid for individual trains but also for the whole train traffic.

Keywords

Steel railway bridge, distortion-induced fatigue, strain measurements

1 Introduction

Both, steel and composite bridges are susceptible to fatigue failure. Detected fatigue cracks at existing bridges are commonly distortion-induced. The reason for distortion-induced fatigue cracks are partially restrained out-of-plane deformations of individual cross-section parts, leading to high secondary stresses. For bridge girders this may particularly occur at the web gap region, if transverse stiffeners are not directly connected with the flanges. Due to out-of-plane deformations of the web plate, large bending stresses in vertical direction may occur. These may result in horizontal fatigue cracks at the main girder web, between the weld toe of the vertical stiffener and the main girder flange. Research related to distortion – induced fatigue, also related to bridges, can be found in [1-8].

Within this paper, the local fatigue behaviour of a specific connection detail in an existing railway bridge, between the main girder flange and the transverse web stiffener is analysed. Fig. 1 shows this detail, which was commonly used for welded railway bridges in Austria during the 1950s and 1970s, because this type of constructional detail was also recommended in the national design code [9]. A fitting strip was situated below the transverse stiffener – only welded to the stiffener itself, but not to the main girder flange. In addition, cut-out holes were used between the stiffener end and the web plate, which result in a small unstiffened web gap where horizontal fatigue cracks were detected at some stiffener connections during regular inspection. Fig. 2 shows one typical example for

https://doi.org/10.1002/cepa.2392 wileyonlinelibrary.com/journal/cepa

the detected fatigue cracks, with a maximum overall crack length of L = 50 mm. The basic idea behind this construction detail was to improve the fatigue resistance of the main girder, with the weld toe of the vertical stiffener now terminating in the web, where the normal stresses due to global bending are significantly reduced. Fig. 2 also indicates the relevant hot spot (hs) in the web plate at the weld toe of the stiffener weld.

The orientation of the observed cracks in longitudinal direction of the girder indicates high local vertical stresses σ_z in addition to the stresses σ_x due to the global behaviour of the main girder. Within a research project for the owner of the railway bridge (ÖBB) comprehensive strain measurements in service and material tests (including fracture test for determination of fracture toughness K_{Ic} and crack growth parameters C, m) were done. Based on these measurements, fracture mechanics analyses showed sufficient remaining fatigue life [10]. Only as an immediate action, stop holes were executed at each detected crack tip, but no restriction in service was necessary.

The main focus of this paper is the presentation of three different reinforcements for this specific type of connection detail. The efficiency of these reinforcements in comparison with the original detail is shown, based on strain measurements for the passage of representative trains.

2 Studied bridge structure

The studied bridge, see Fig. 1, consists of two individual structures, each for one track of a railway main line in Austria. Each structure has two main girders with three continuous spans. They are connected by cross bracings at every second position of the transverse stiffeners along the bridge, with stiffeners at both sides of the main girder web. The specific connection between the transverse stiffeners and the main girder, already discussed in the previous section, is also shown in Fig. 1.

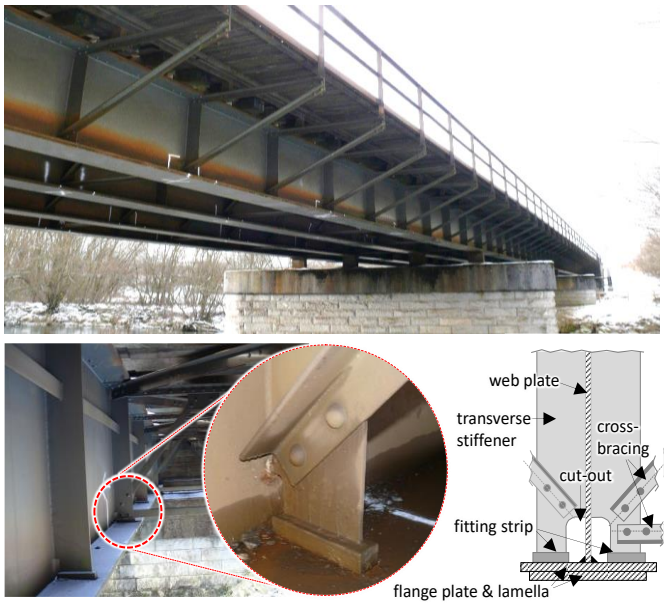

Figure 1 Studied railway bridge with welded main girders and specific transverse stiffener connections

The sleepers of the track are situated directly at the top of the main girders. The span length of the main girders is L = 21 m, with a depth of h ≈ 1300 mm, leading to a slenderness ratio of L/h = 16. The dimensions of the flanges are b/t = 500/24 and 500/30 (main span) with lamellas 460/16 on both flanges in the side spans. The thickness of the web varies between t_w = 8-12 mm. The distance between the transverse stiffeners in longitudinal direction is e_{st} = 1,75 m, leading to a distance of e_{cb} = 3,50 m of the cross bracings. The dimensions of the transverse stiffeners and the fitting strip are 200/20 and 40/40 mm.

The bridge was built in the 1960s, with fully welded main girders and riveted site joints. Steel quality St 44 T was used, with a nominal yield stress of approximately f_y = 284 $\mathrm{N/mm^2}$. This could be confirmed by the latest results of four tensile coupon tests for the main girder web, with a mean value $f_{y,m}$ = 305 $\mathrm{N/mm^2}$ and $f_{u,m}$ = 478 $\mathrm{N/mm^2}$ for the ultimate tensile strength.

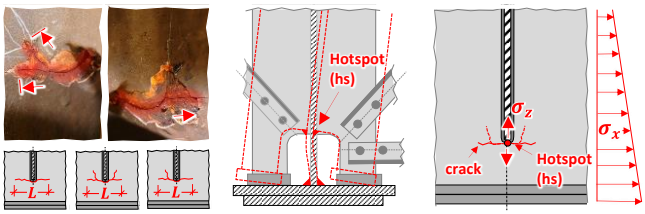

Figure 2 Observed crack pattern at the specific transverse stiffener connections

To assess the fatigue damage, due to the local stress field only, the fatigue resistance (of the local effect only) was determined, based on results in the literature. The procedure to assess the local stress spectra and the local fatigue damage respectively for the original detail and the three different reinforcements is presented. In a first step this is shown for the two representative trains. Afterwards a prediction of the local fatigue damage of all three reinforcements for all service trains is shown.

These results allow also a prediction of the three developed reinforcements for other railway bridges at main lines of ÖBB.

3 Measurements of the local stress field at the specific connection detail

Before, specifying five representative connection details (overall 140 details, that means 35 at each main girder) for detailed measurement of the local stress field, the global fatigue damage at the hot spot was calculated, based on the train mix in EN 1991-2 for fatigue design. These calculations showed a significant higher fatigue damage, due to the global behaviour, in the side spans. In contrast, the detected fatigue cracks were not only detected in the side spans, but also in the centre span. Only at the connection details with cross bracings, fatigue cracks were found. The extent of damage was very similar for all four main girders. This was in accordance with the statistical data of the train service, with nearly the same traffic volume on both tracks.

Therefore the strain measurements were only done on the two main girders of one track at a location in the side span and one in the centre span, where at one main girder cracks were detected and at the other not. In addition, one connection detail without cross bracing was selected. For

application of fracture mechanics, to predict the crack growth starting at the hot spot, the local stress field around the hot spot is essential. Therefore, not only strain gauges were used, but also strain gauge rosettes (details in [10]). The analyses of the measured local stress fields showed, that only the vertical stresses $\sigma_{z,hs}$ are necessary to predict, whether a fatigue crack will start or not.

Therefore, for the assessment of the individual reinforcements only the vertical stresses $\sigma_{z,hs}$ are necessary. It is important to use the measured stresses $\sigma_{z,hs}$ at a connection detail without any fatigue crack, because cracking leads to a reduction of the local stresses [10]. Fig. 3 shows the position of the individual strain gauges on both surfaces of the web plate, which allow an extrapolation of the stress $\sigma_{z,hs}$ at the hot spot at the weld toe. Within this paper only the results for the connection detail at position P2 without fatigue cracks, at the side span of main girder MG 4, are shown.

In addition, the clearance between the lower flange of the girder and the fitting strip of the transverse stiffener was measured, at both sides of the girder web, in vertical and horizontal direction (Fig. 3).

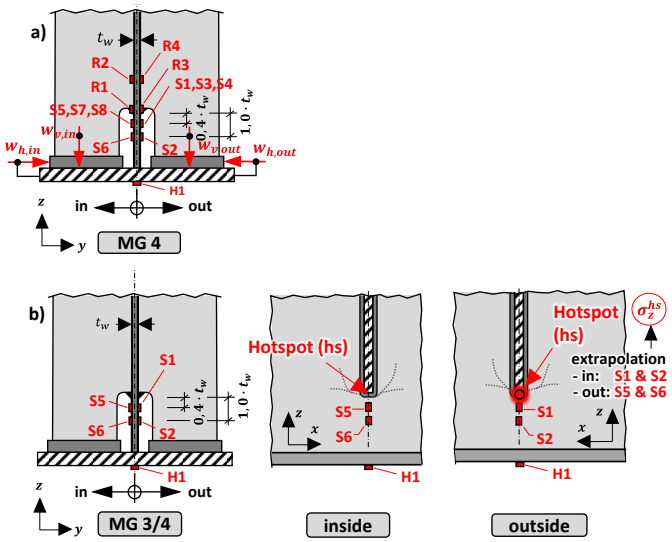

Figure 3 a) measurements of the clearance between fitting strip of the transverse stiffener and girder flange; b) Position of strain gauges to predict the stresses $\sigma_{z,hs}$ at the hot spot

4 Presentation of the developed reinforcements

The following requirements are essential for the design of reinforcements at the specific connection detail:

- no additional welds at the main girder (e.g. between fitting strip and girder flange), to prevent a reduction of the fatigue resistance of the main girder
- avoidance of holes at the main girder and separating cuts of bracing elements, in order to keep the full cross section capacity of the main girder. Based on this, no structural analyses are needed and during erection no interruption of train service is required
- reduction of reinforcement efforts recommended in the literature, in cases of distortion-induced fatigue failure (reinforcement angles with bolted connections to flange and vertical stiffener)

Fig. 4 shows the developed three variants of reinforcement for the specific constructional detail. Variant R1 only needs filler plates below the fitting strips of the transverse stiffeners (in and outside of the web plate). Variant R2 is a clamped solution only, needing no holes at the main girder. At the upper part of the girder flange, the two vertical plates at both sides of the transverse stiffener, have a welded cleat. These cleats are pushing on the fitting strip when the screws are preloaded (four bolts necessary on both sides of the girder flange).

Variant R3 also has welded cleats at the angle members, only on the upper side of the girder flange. In this bolted solution only a bolted connection to the girder flange is needed, with prestressed bolts. For variant R2 and R3 also filler plates, as for variant R1, are needed.

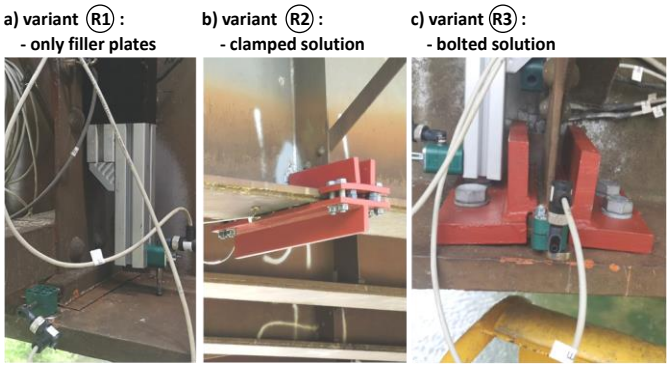

Figure 4 Developed reinforcements of the specific constructional detail; a) variant R1 with filler plates only; b) variant R2 – clamped solution; c) variant R3 – bolted solution (all bolts are pre-tensioned)

5 Efficiency of the reinforcements based on measurements under train operation

At all measuring sensors (see Fig. 3) permanent measurements were done under regular train service over a period of two weeks. Within these two weeks, measurements were done at least for some days at, i) the original constructional detail, ii) reinforcement variant R1, iii) reinforcement variant R2 and iv) reinforcement variant R3.

Within this measurement period also a weigh-in-motion-device was installed at the rail behind the abutment, to get the individual train characteristic (distance and weight of individual axles, train velocity, total train weight).

To get an overview of the detail performance, first of all only the maximum and minimum value of each sensor, during train passage, was detected. Fig. 5 shows these results for the vertical and horizontal clearance below the transverse stiffener. Each train is specified with an orange and a blue dot. For a representative passenger train (called Railjet) and freight train the results are marked in red and black. The most important result is the extremely small change of clearance, also at the original detail. During one train passage the change of clearance is about $\Delta w \approx 0{,}2$ mm. The efficiency of the individual reinforcement variants is visible. Already variant 1 with the filler plates showed a significant better performance and variant R2 (clamped solution) shows nearly the same good performance, than variant R3 (bolted solution).

For assessment of the local fatigue damage only maximum

and minimum stresses $\sigma_{z,hs}$ are not sufficient and the stress-time history is needed. In addition, for an objective comparison between original constructional detail and each reinforcement variant always the same trains should be used. With the help of the weigh in motion device it was possible to pick out one representative passenger train (Railjet) and also one representative freight train (trains not exactly the same, but similar axle weights and number of axles).

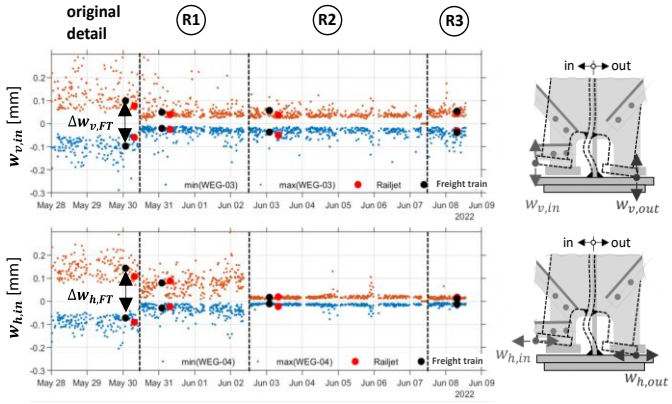

Figure 5 Measured maximum and minimum clearance during one train passage; results for the original detail and all three reinforcement variants

Fig. 6 shows the stress-time history for the passage of the passenger train.

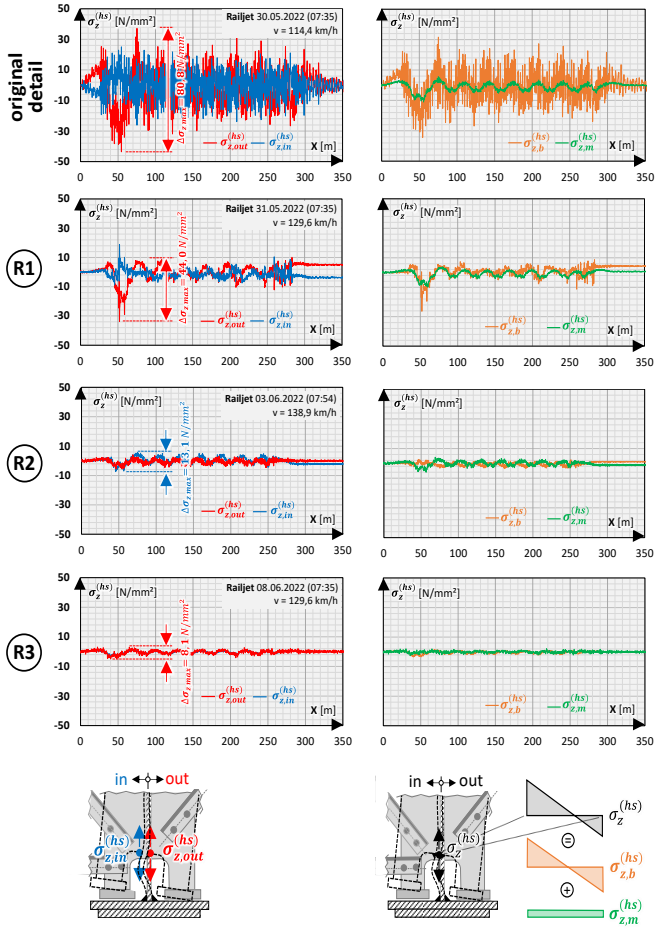

Figure 6 Stress-time histories for the local stresses $\sigma_{z,hs}$ at the hot spot for the passage of the passenger train (Railjet); results for the original detail and all three reinforcement variants

The results for the freight train are very similar, despite the significant lower train velocity. The figures on the left show the results at the two hot spots, at both surfaces of the girder web (blue and red line). The figures on the right show, that the membrane stresses (green lines) are very small, compared to the dominating bending stresses, as expected for distortion-induced fatigue failure. For the original detail an unexpected effect, based on the results in the literature, can be seen. The bending stresses show the effects of a resonance vibration of the web plate, with a measured frequency of $f_{\sigma z} \approx 20$ Hz, significantly higher than the natural frequency of the main girder in bending. Already with reinforcement variant R1 the stress cycles $\Delta\sigma_z$ are significantly reduced and also the vibration effects disappear. The reinforcement variants R2 and R3 again improve the performance and lead to similar results with very small stress cycles.

Based on the stress-time history in Fig. 6, with Rainflow-method the individual stress cycles were calculated and summed up in stress spectra. Fig. 7 shows these stress spectra for the passage of the passenger train and freight train respectively for both hot spots (on each side of the web plate). The stress spectra are shown for the original detail as well as for the three reinforcement variants.

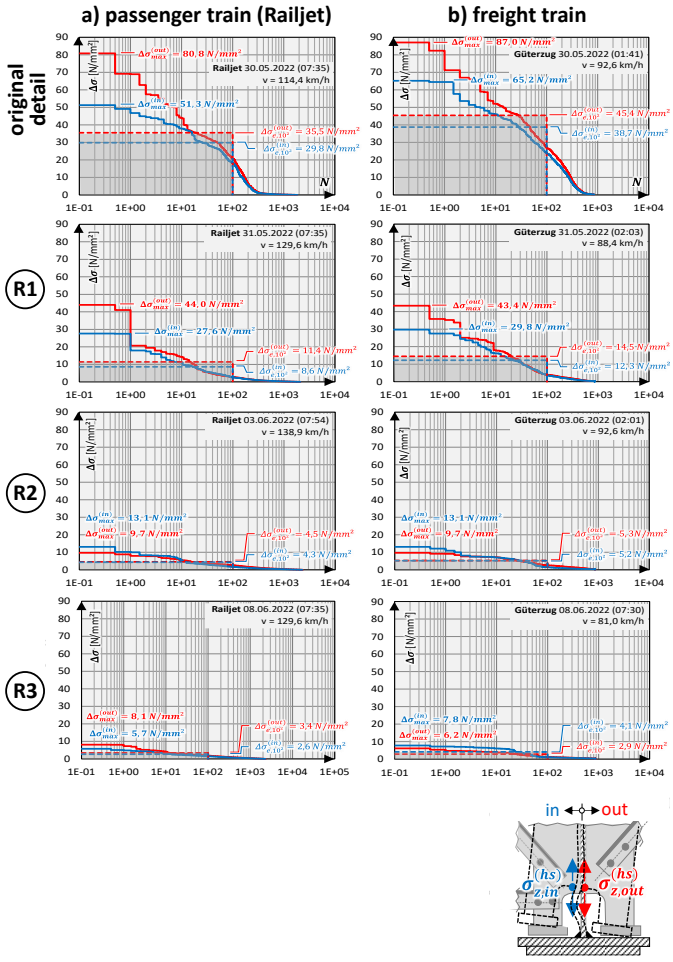

Figure 7 Stress spectra for the local stresses $\sigma_{z,hs}$ at the hot spot for the passage of: a) one passenger train, b) one freight train; results for the original constructional detail and all three reinforcement variants

Table 1 shows the measured reduction factors of the maximum stress cycles $\Delta\sigma_{max,ori}$ of the original detail for the three individual reinforcement variants. The passage of

the passenger train shows slightly higher values, than the passage of the freight train and these former results were used for the assessment of the overall stress spectra due to regular train service (measurement for eight weeks on the original constructional detail). Table 1 in addition shows also the reduction factor for the damage equivalent stress cycle $\Delta\sigma_e$, indicating similar values. The reduction factors for the maximum stress cycles $\Delta\sigma_{max,ori}$ for each reinforcement variant are applicable as an approximation also for the individual stress cycles $\Delta\sigma_{i,ori}$. For this reason the measured stress spectra of the original detail, multiplied with the reduction factors of Table 1, lead to the stress spectra of the individual reinforcement variants.

Table 1 Reduction of the maximum stress cycles $\Delta\sigma_{max,ori}$ of the original detail for the individual reinforcement variants due to representative train passage (reduction factors $f_{\sigma,Ri}$)

	crossing **passenger train (Railjet)**				crossing **freight train**			
	$\Delta\sigma_{max}$ [N/mm²]	$\frac{\Delta\sigma_{max}}{\Delta\sigma_{max,ori.}}$	$\Delta\sigma_{e,10^2}$ [N/mm²]	$\frac{\Delta\sigma_{e,10^2}}{\Delta\sigma_{e,10^2,ori.}}$	$\Delta\sigma_{max}$ [N/mm²]	$\frac{\Delta\sigma_{max}}{\Delta\sigma_{max,ori.}}$	$\Delta\sigma_{e,10^2}$ [N/mm²]	$\frac{\Delta\sigma_{e,10^2}}{\Delta\sigma_{e,10^2,ori.}}$
original detail	80,8	1,00	35,5	1,00	87,0	1,00	45,4	1,00
R1	44,0	**0,54**	11,4	0,32	43,4	**0,50**	14,5	0,32
R2	13,1	**0,16**	4,5	0,13	13,1	**0,15**	5,3	0,12
R3	8,1	**0,10**	3,4	0,10	7,8	**0,09**	4,1	0,09

reduction of $\Delta\sigma_{max}$ and $\Delta\sigma_i$

6 Assessment of the reinforcement variants for train service in general

Based on the shown strain measurements for representative passenger and freight trains for the original detail, as well as for the three reinforcement variants, stress reduction factors were developed (see Table 1). The measured stress spectra at the original detail include the overall train service for a main line of ÖBB in Austria and were extrapolated for one year of service (route data showed that eight weeks of measurement are adequate to extrapolate for one year of service). With the stress reduction factors $f_{\sigma,Ri}$ for each reinforcement variant the stress spectra for the overall train service is available for the final fatigue assessment.

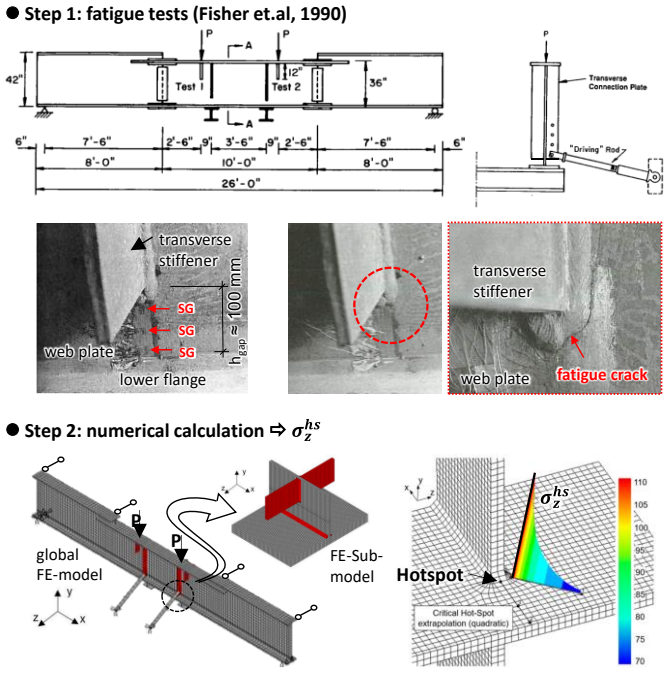

Figure 8 Fatigue tests to determine the fatigue strength at the constructional detail for the local fatigue effect only

To quantify the local fatigue damage at the hot spot of the investigated constructional detail, an accurate fatigue strength, for the local effect only, is necessary.

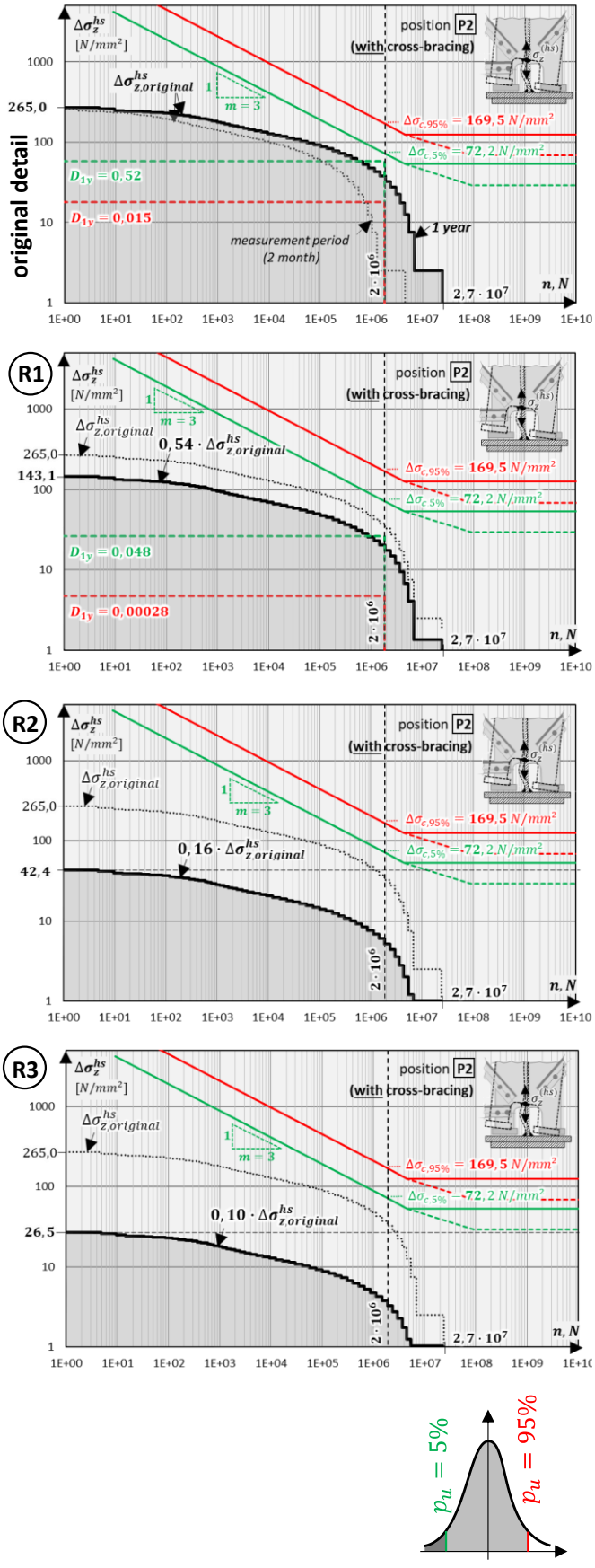

Figure 9 Final assessment of the three reinforcement variants based on the stress spectra (for one year of service) of overall train service and accurate SN-curve for the local fatigue effect only

Based on the fatigue tests of Fisher et.al [11] and the exchange of these fatigue strength values in the concept of the hot spot stress method [12] these fatigue strength values are available, see Fig. 8. Based on EN 1990, Annex D design values of the fatigue strength of the local effect were calculated for the final assessment of all three reinforcement variants. Fig. 9 shows the stress spectra for one year of service and the design curves for the fatigue strength (CAFL at $N=5\cdot10^6$, based on EN 1993-1-9, is also shown) for the original detail as well as for all three reinforcement variants. The low design fatigue strength of $\Delta\sigma_{c,5\%}$.= 72,2 N/mm^2, compared with the design regulations for the hot spot stress method in EN 1993-1-9 [13] ($\Delta\sigma_{c,hs}$.= 100), is based on the small number of tests in [6], with high scatter.

The high stress cycles $\Delta\sigma_{z,hs}$ of the local fatigue effect at the original detail, with a calculated local fatigue damage of $D_{ori,1year}$ = 0,52 for one year of service, also indicates the detected fatigue cracks after approximately 60 years in service.

The reinforcement variant R1 with only filler plates shows a significant reduction of the local fatigue damage ($D_{R1,1year} \approx$ 0,05), but is not adequate to guarantee no fatigue cracks within the service life of the bridge. Because the efforts for this type of reinforcement are very small it should be applied as an immediate measure. It also should improve the corrosion protection at this constructional detail (closing the open gap below fitting strip).

The reinforcement variant R2 (clamping solution) and R3 (bolted solution) lead to maximum stress cycles below the constant amplitude fatigue limit (CAFL). But, due to the higher stress cycles in the past, acting on the original detail and leading to pre-fatigue damage, this verification is not sufficient. The fatigue limit for variable amplitude stress cycles must be considered in this case, leading to a reduced design value of $\Delta\sigma_L$= 29,2 N/mm^2, according to the SN-curves in EN 1993-1-9 [13]. Therefore, for variant R3 the local damage at the hot spot in the future is negligible and only the global fatigue damage at the constructional detail must be considered. Looking at the higher fatigue strength for the hot spot stress method in EN 1993-1-9 [13] ($\Delta\sigma_{c,hs}$= 100), with an increased design value of $\Delta\sigma_L$= 40,5 ≈ $\Delta\sigma_{max}$= 42,4 N/mm^2, also reinforcement variant R2 seems sufficient to prevent significant local fatigue damage in the future.

Due to the very beneficial behaviour of the developed three reinforcement variants for this kind of specific constructional detail also an application at other railway bridges seems useful.

7 Acknowledgements

The presented research activities are part of a COMET-research project called Rail4Future, organised by ÖBB-Infrastructure (provider of the Austrian railway system), in the area of reliable bridge structures. The authors would like to thank ÖBB for the financial support as well as the following persons for their cooperation and support: Heissenberger M., Hüngsberg A., Forstlechner F., Gasparin G., Gross E. and Vospernig M.

References

[1] Fisher J.W.; Keating P.B.: Distortion-induced fatigue cracking of bridge details with web gaps, Journal of Constructional Steel Research; Vol. 12: 215-228, 1989

[2] Skoglund O.; Leander J.: Distortion induced fatigue of web-gap details, a parametric study, Engineering Structures; Vol. 254, Issue 9, 2022

[3] Aygül M.; Al-Emrani M.; Barsoum Z.; Leander J.: Investigation of distortion-induced fatigue cracked welded details using 3D crack propagation analysis, International Journal of Fatigue; Vol. 64: 54-66, 2014

[4] Al-Emrani M.: Fatigue performance of stringer-to-floor-beam connections in riveted railway bridges, Journal of Bridge Engineering; Vol. 10: 179-185, 2005

[5] Jajich D.; Schultz A.E.: Measurement and Analysis of Distortion Induced Fatigue in Multigirder Steel Bridges, Journal of Bridge Engineering, Vol. 8: 84-91, 2003

[6] Fisher, J.W.; Jin J.; Wagner D.: Distortion induced fatigue cracking in steel bridges, NCHRP Report No. 336, National Cooperative Highway Research Program, Urbana, Issue 11, 1990

[7] Dellenbaugh L.; Kong X.; Al-Salih H.; Collins W.; Bennett C.; Li J.; Sutley E.J.: Developement of a Distorion-Induced Fatigue Crack Characterization Methodology Using Digital Image Correlation, Journal of Bridge Engineering; Vol.25, 1990

[8] D'Andrea M.; Grondin G.Y.; Kulak G.L.: Behaviour and rehabilitation of distortion induced fatigue cracks in bridge structures, Structural engineering report No. 240, Department of Civil and Environmental Engineering, University of Alberta, Alberta, 2001

[9] ÖNORM B4600-7: Ausführung von Stahltragwerken, Austrian Standard Institute, Vienna, 1964

[10] Derler C., Unterweger H., Distortion-induced fatigue failure at main girders of a railway bridge – strain measurements in service and analyses based on fracture mechanics, in: SDSS 2022, Aveiro/Portugal, Int. Colloquium on Stability and Ductility of Steel Structures, 14th – 16th September 2022, Proceedings, 10 pages, September 2022.

[11] Fisher, J.W.; Jin, J.; Wagner, D.C.; Yen, B.T. NCHRP Report 336: Distortion-Induced Fatigue Cracking in Steel Bridges; National Research Council of Washington: Washington, DC, USA, 1990.

[12] Quissanga, V.; Alencar, G.; de Jesus, A.; Calcada, R.; da Silva, J.G.S: Distortion-Induced Fatigue Reassessment of a Welded Bridge Detail Based on Structural Stress Methods; in: Metals, Vol. 11, 2021

[13] EN 1993-1-9; Eurocode 3: Design of steel structures – Part 1-9: Fatigue, CEN, Brussels, 2010